DALTON
FULL PAPER

Synthesis, structure and thermal stability of tellurium oxides and oxide sulfate formed from reactions in refluxing sulfuric acid †

Mohammad A. K. Ahmed, Helmer Fjellvåg and Arne Kjekshus

Department of Chemistry, University of Oslo, P.O. Box 1033, Blindern, N-0315 Oslo, Norway

Received 7th July 2000, Accepted 16th October 2000
First published as an Advance Article on the web 28th November 2000

Reactions between Te, TeO_2, $TeCl_4$, TeO_3 or H_6TeO_6 and 30–95 wt% H_2SO_4 were studied at temperatures up to the boiling point of the acid. Depending on the tellurium-containing reactant, H_2SO_4 concentration and synthesis temperature, $Te_2O_3(SO_4)$, TeO_3 or $TeO_3{\cdot}xH_2O$ (x = 1.37–1.58) is obtained as the final product (alone or in admixture). The reaction products as well as thermally decomposed and/or crystallized/recrystallized products of these are characterized by powder X-ray diffraction and thermoanalytical techniques. The findings obtained by syntheses with, and thermal decompositions of, H_6TeO_6 concern three crystalline [TeO_3 (I), TeO_3 (II) and TeO_3 (III) in the present notations] and one amorphous modification of TeO_3, an amorphous modification of H_2TeO_4, one crystalline and one amorphous modification of $TeO_3{\cdot}xH_2O$ (x = 1.37–1.58) and two crystalline (one with somewhat more uncertain composition) and one amorphous modification of Te_2O_5. The crystal structures of TeO_3 (I) and $Te_2O_3(SO_4)$ have been redetermined by Rietveld refinements of powder X-ray and neutron diffraction data, respectively.

Introduction

The present contribution on synthesis, structure and thermal stability of tellurium oxides and oxide sulfate represents a continuation of our earlier published work on corresponding phases of iodine,[1–5] titanium,[6] tin,[7] zirconium,[8] hafnium[8] and molybdenum.[9,10] Owing to its position in the Periodic Table the chemistry of tellurium is relatively unique among the elements. Over the years a considerable amount of work has been devoted to studies of tellurium oxides, oxo acids and halides (see Refs. 11,12) whereas other fields of tellurium chemistry are less studied.

Two ambient-pressure, crystalline forms of tellurium dioxide have been prepared (one corresponding to the mineral paratellurite,[13–16] and the other to the mineral tellurite[17,18]) in addition to a high-pressure phase.[19,20] A recent survey[21] establishes 733 ± 1 °C as the melting point of tellurium dioxide, whereas the phase diagram in the vicinity of this point is not known. It has been suggested[21,22] that Te_4O_9 is not a proper tellurium oxide but rather an oxide hydrate. The hydrothermal[23] synthesis of Te_4O_9 from H_6TeO_6, TeO_2 and water could lend support to this suggestion. However, the structure determination[24] did not reveal significant amounts of H_2O in the Te_4O_9 lattice. Te_4O_9 is also obtained[22] (in admixture with Te_2O_5 and TeO_2) by heat treatment of amorphous TeO_3 at 450–500 °C. The onset of the thermal decomposition of Te_4O_9 is listed[21] at some 500 °C, and the final product obtained at 650 °C is phase-pure TeO_2.[23] Thermal decomposition of H_6TeO_6 or TeO_3 at 400–450 °C is said[22,25] to give Te_2O_5, and suitable single crystals for structure determination[26] have been obtained (together with TeO_3) hydrothermally from H_6TeO_6 and water. At constant temperature the onset of the thermal decomposition of Te_2O_5 to TeO_2 is listed[21] at 500–520 °C (see also Refs. 22,27), the decomposition rate being appreciable at 595 °C.[21,22]

One amorphous and two crystalline modifications of TeO_3 are described in the literature[21,22,28–37] but only one of the crystalline forms is characterized by structure determination (FeF_3 type).[32,37] The synthesis route to the latter modification usually involves thermal decomposition of H_6TeO_6 (or H_2TeO_4) with small variations in the details of the procedure; sealed[28–32,35,37] *vs.* open[22] ampoule, with[22,29,30,32,35] or without[36] added H_2SO_4 and a certain span in the applied temperature (300–350 °C) and the duration of the treatment (3–200 h). According to Ref. 33 this modification of TeO_3 can not be prepared in an open system in air. The second crystalline modification is prepared[30] by heat treatment of amorphous TeO_3 at *ca.* 300 °C for 12–36 h. This form is characterized by powder X-ray diffraction data (d values and relative intensities) and its synthesis has apparently been reproduced in Ref. 31. Amorphous TeO_3 is obtained[25] by thermal decomposition of H_6TeO_6 at 310 °C in air and at nearly the same temperature in 0.1 Pa vacuum,[22] the latter product being formulated as $TeO_3{\cdot}xH_2O$ (x = 0.01–0.15). The thermal decomposition sequence of H_6TeO_6 has frequently been studied[22,25,34,36,38–41] and it appears to be a reasonable consensus that H_2TeO_4, TeO_3 and Te_2O_5 occur as intermediates of this degradation, and that TeO_2 is the final oxide product (see above). However, other intermediates have also been introduced; *viz.* $(H_2TeO_4)_n{\cdot}H_2O$,[34] $H_2Te_2O_7$,[34] $xTeO_3{\cdot}yTeO_2{\cdot}zH_2O$,[34] $uTeO_2{\cdot}TeO_3$,[34] $TeO_x{\cdot}yH_2O$ (x = 2.4–3.1, y = 0.0–0.5),[33] Te_4O_{11}[36] and Te_4O_9.[36] The crystal structures of four tellurium oxo acids [$H_2Te_2O_6$,[42] H_6TeO_6(monoclinic),[43,44] H_6TeO_6(cubic),[45] and H_2TeO_4[46]] are well established.

An account of the (early) preparation history of $Te_2O_3(SO_4)$ is given in Gmelin,[47] the easiest recipe being to heat TeO_2 in conc. H_2SO_4. More recent studies have focused on its structural properties.[35,48–52] Its structure consists of Te_2O_3 layers parallel to (001). The layers are connected through sulfate groups which are bound more closely to one of the adjacent layers. However, mutual disagreements between Refs. 50–52 have been pointed out.[53] $Te_2O_3(SO_4)$ is reported to decompose to TeO_2 at 345–450 °C on heating,[48] the temperature being clearly very dependent on the heating procedure and the surrounding atmosphere. The main content of this paper concerns the mutual relationships between many of these phases as a function of sulfuric acid concentration and temperature. In addition we report on thermally decomposed and/or

† Electronic supplementary information (ESI) available: PXD data for $TeO_3{\cdot}xH_2O$ and TeO_3 (III). See http://www.rsc.org/suppdata/dt/b0/b005688j/

 DOI: 10.1039/b005688j

crystallized/recrystallized products, and crystal structure refinements for TeO_3 (I) and $Te_2O_3(SO_4)$.

Experimental

Syntheses

Telluric acid [H_6TeO_6 Fluka, 99%; monoclinic, $a = 649.34(5)$, $b = 931.90(6)$, $c = 833.09(6)$ pm, $\beta = 99.682(6)°$], TeO_2 [Fluka, pract., >95%; tetragonal, $a = 481.11(3)$, $c = 761.04(7)$ pm], $TeCl_4$ (Alfa, 99%), tellurium powder [Fluka, purum, >99.7%; hexagonal, $a = 445.74(5)$, $c = 592.8(1)$ pm], and conc. H_2SO_4 (Merck, p.a.; 95–97 wt%, the former value being used throughout this paper) were used as starting chemicals for the syntheses. H_2SO_4 concentrations in the range 30–95 wt% were made by diluting with distilled water.

With H_6TeO_6 as starting chemical, 50 ml conc. H_2SO_4 [originally 95 wt%; in some cases first heated at 320–325 °C for *ca*. 2 h (open system) to increase the concentration towards 100 wt% H_2SO_4] and 4.6 g of telluric acid were mixed. Such mixtures were stirred in a round-bottomed flask equipped with a reflux cooler at temperatures from room temperature (r.t.) to boiling point (bp) for 1 d or longer. After cooling to r.t. (with frequent intermediate stirring in order to avoid mass solidification and sticking of the product to the glass of the reaction vessel) a white–yellowish, non-hygroscopic precipitate was obtained. Similar syntheses gave white products for reactions in 60–75 wt% H_2SO_4 and white–yellowish products for 80–95 wt% H_2SO_4. The liquid phase was removed by decantation and the precipitate stirred with *ca*. 100 ml glacial acetic acid for 15 min, filtered off, and washed with glacial acetic acid and acetone. The entire washing procedure was repeated twice before the product was dried and stored in a desiccator.

A similar procedure was followed with tellurium dioxide as starting chemical. 3.2 g TeO_2 and 30–95 wt% H_2SO_4 (50 ml) were treated for periods of 1–2 d. After cooling to r.t., the colourless to yellowish clear liquid phase was removed by decantation. The white precipitate was treated as described above. In the case of tellurium tetrachloride as starting chemical, 8.1 g $TeCl_4$ were similarly treated with 50 ml 60–95 wt% H_2SO_4 in the described reaction system. With tellurium powder as starting chemical, mixtures of 5.1 g Te and 50 ml 60–95 wt% H_2SO_4 were heated and stirred at different temperatures (from r.t. to bp) for reaction periods of 2 h to one week, depending on acid concentration and temperature, usually judged by the amount of deposited white, non-hygroscopic precipitate in the colourless solution.

Duplicate experiments at r.t. were performed by treating tellurium powder with 95 wt% H_2SO_4 for one week, as described above. The stirring was then stopped and the liquid and solid phases were separated by filtering through a sintered-glass funnel. The obtained violet solution was added to 150 ml glacial acetic acid with stirring, and a bulky black precipitate immediately separated. The solid product was filtered off, washed with glacial acetic acid and dried in a desiccator. The small amount of white solid product remaining on the sintered-glass funnel was washed with 95 wt% H_2SO_4 until no violet colouring of the washing liquid could be seen, and then washed with glacial acetic acid and dried in a desiccator.

Precipitated TeO_3 was purified by washing with a concentrated KOH solution and thereafter with distilled water. Afterwards it was washed with concentrated HCl and subsequently with distilled water (until pH *ca.* 6). The products after filtering were dried at 300 °C.

Powder X-ray and neutron diffraction and refinements

Characterization by powder X-ray diffraction (PXD) was performed with Guinier–Hägg cameras (Cu-Kα1 radiation, Si as internal standard). Positions of Bragg reflections were obtained by means of a Nicolet L18 scanner using the SCANPI program system.[54] Indexation of unknown diffraction patterns was attempted using the TREOR program.[55] Unit-cell parameters were refined using the CELLKANT program.[56]

PXD intensity data for the refinement of the TeO_3 (I) crystal structure were collected with a Siemens D5000 diffractometer equipped with primary germanium monochromator, position sensitive detector, using Cu-Kα1 radiation and the sample in cylinder (transmission) geometry.

Powder neutron diffraction (PND) data for $Te_2O_3(SO_4)$ were collected with the high-resolution, two-axis diffractometer PUS at the JEEP II reactor, Kjeller, Norway. Monochromatized neutrons of wavelengths 155.4 pm were obtained by reflections from Ge(511) and detected by two PSD banks, each covering 20° in 2θ. Diffraction data were measured at r.t., between $2\theta = 10$ and 130°, and analysed in steps of $\Delta 2\theta = 0.05°$. A cylindrical sample holder was used and filled with *ca.* 1.5 g sample.

Rietveld refinements of the PXD and PND data were performed with the program GSAS.[57] A pseudo-Voigt profile function was used both for the PXD and PND data. Isotropic thermal parameters were refined individually for the elements of different kinds but no absorption correction was made.

Thermoanalyses

Thermogravimetric (TG) and differential thermal (DTA) analyses were performed between 20 and 800 °C with a Perkin-Elmer TGA 7 and DTA 7 system, respectively. The 15–40 mg samples were placed in Al_2O_3 crucibles, nitrogen was used as atmosphere and the heating rate was 10 °C min^{-1}.

Table 1 Solid products synthesized at different temperatures by reaction between H_6TeO_6 and H_2SO_4 in different concentrations

wt% H_2SO_4	*T*/°C	Product
30–55	r.t.–136 (bp)	H_6TeO_6
95	r.t.	H_6TeO_6
95	135	$TeO_3 \cdot xH_2O$, $x = 1.58$; amorphous
60–75	150–190 (bp)	$TeO_3 \cdot xH_2O$, $x = 1.37$–1.58; crystalline
95	200	TeO_3 (III); 5 wt% adsorbed H_2O
80–95	210–290 (bp)	TeO_3 (III); 2–5 wt% adsorbed H_2O
ca. 100	250	TeO_3 (II); 2 wt% adsorbed H_2O
ca. 100	320	TeO_3 (I); 2 wt% adsorbed H_2O

Results and discussion

Telluric acid (H_6TeO_6) as reactant

H_6TeO_6 as reactant in 60–*ca.* 100 wt% H_2SO_4 leads to at least four different solid reaction products [Table 1; TeO_3 (I), TeO_3 (II), TeO_3 (III) and $TeO_3 \cdot xH_2O$ (in two forms, crystalline and amorphous, $x = 1.37$–1.58), arranged according to decreasing concentration of H_2SO_4 and reaction temperature]. (In order to avoid confusion with the literature where the designations A, B, C, α, β and γ have been used to name different modifications of TeO_3, the notations I, II and III are used to distinguish those prepared in this study.) The yields were generally good for syntheses in 95 wt% H_2SO_4 between 200 °C and bp, but lower for less concentrated acid. For reaction temperatures below 200 °C (even for 95 wt% H_2SO_4) the products became X-ray amorphous and contained appreciable amounts of water. For reactions attempted at r.t. the solid "product" proved to be unchanged H_6TeO_6, but the low residual indicates some dissolution of H_6TeO_6 in 95 wt% H_2SO_4.

As the concentration of H_2SO_4 was decreased the particle size of the solid products decreased (recognized by PXD) and their water contents increased gradually (see Table 1). The H_2SO_4 concentration and the reaction temperature play a decisive role for the product obtained, in particular with respect to the different forms of TeO_3.

Table 2 Unit-cell dimensions at r.t. with e.s.d.s in parentheses for tellurium–oxygen-containing compounds

Compound	Symmetry	*a*/pm	*b*/pm	*c*/pm	*α*/°	*β*/°	*γ*/°	*V*/10⁶ pm³	*M*(20)[a]
H_6TeO_6 [21,22]	Monoclinic	649.34(5)	931.90(6)	833.09(6)		99.682(6)		496.94(6)	192.9
H_2TeO_4	Amorphous								
$TeO_3{\cdot}xH_2O$	Unindexed								
$TeO_3{\cdot}xH_2O$	Amorphous								
TeO_3 (I) [18,19]	Rhombohedral[b]	519.47(1)			56.38(8)			272.45(6)	
TeO_3 (II)	Hexagonal	515.0(1)		1429.6(19)				328.4(5)	
TeO_3 (III)	Unindexed								
TeO_3 (IV)	Amorphous[c]								
Te_2O_5 (I) [17]	Monoclinic[c]	537.0(2)	469.5(1)	795.7(3)		104.79(3)		194.0(1)	65.1
Te_2O_5 (II)[d]	Triclinic[c]	431.7(1)	593.2(1)	876.7(1)	57.35(1)	78.71(1)	90.54(1)	183.54(5)	346.1
Te_2O_5 (III)	Amorphous[c]								
Te_4O_9 [16]	Hexagonal[c]	932.49(5)		1449.2(2)				1091.3(2)	108.8
$Te_2O_3(SO_4)$ [25–27]	Orthorhombic[e]	888.20(3)	693.57(2)	465.39(1)				286.66(6)	135.9
α-TeO_2 [9–12]	Tetragonal[c]	481.11(3)		761.04(7)				176.15(3)	305.1
β-TeO_2 [13]	Orthorhombic[f]	1206.1(6)	546.5(3)	560.1(2)				369.5(3)	23
γ-TeO_2	Unindexed[f,g]								

[a] Figure of merit. [b] Diffractometer data: hexagonal setting, $a = 490.77(2)$, $c = 1306.2(2)$ pm. Guinier–Hägg data: hexagonal setting, $a = 490.97(4)$, $c = 1306.5(1)$ pm. [c] Obtained by thermal decomposition of H_6TeO_6. [d] The formula may be slightly approximate. [e] Data from PND; PXD gave $a = 887.98(7)$, $b = 693.7(1)$, $c = 465.35(3)$ pm. [f] Obtained from $Te_2O_3(SO_4)$. [g] Obtained in admixture with the α and β modifications.

Characterization by PXD (unit-cell dimensions in Table 2; unindexed diffraction data are deposited as ESI) shows that TeO_3 (I) is identical with the modification described in Ref. 37, also reported as TeO_3 (B)[27,31] and β-TeO_3.[32] TeO_3 (III) has earlier been synthesized by different methods and is reported as TeO_3 (A)[27,31] and γ-TeO_3,[30] but note that our assignment is only based on *d* values. A new modification, TeO_3 (II), was obtained as a crystalline product in our syntheses with *ca.* 100 wt% H_2SO_4 at *ca.* 250 °C.

The hitherto unreported $TeO_3{\cdot}xH_2O$ ($x = 1.37$–1.58) was obtained in crystalline form in syntheses with *ca.* 65–75 wt% H_2SO_4 at 150–190 °C and in an amorphous form with 95 wt% H_2SO_4 at *ca.* 135 °C. TeO_3 (III) and crystalline $TeO_3{\cdot}xH_2O$ occur over comparatively wide concentration and temperature ranges alone and are accordingly easy to prepare. Syntheses of TeO_3 (I) and TeO_3 (II) require attention to the H_2SO_4 concentration and the reaction temperature. All preparations of TeO_3 (I) were contaminated with small amounts of $Te_2O_3(SO_4)$ [increasing with reaction time (when exceeding 3 d) and/or reaction temperature] as a result of the slow decomposition of TeO_3 into TeO_2 which in turn reacts with H_2SO_4 and forms $Te_2O_3(SO_4)$. The oxide sulfate has earlier[48] been obtained from the same reactants in a sealed system.

The progressing reaction between H_6TeO_6 and H_2SO_4 was studied in a simple experiment; 4.5 g H_6TeO_6 were treated with 50 ml 65 wt% H_2SO_4 at bp (*ca.* 150 °C) until a colourless solution was obtained. After cooling to r.t. the still clear solution was divided into two portions. One was added to a flask containing *ca.* 150 ml glacial acetic acid and stirred overnight at r.t. whereby a white precipitate deposited, mainly on the container walls. PXD and TG investigations show that the product after washing and drying actually is H_6TeO_6. The second portion was heated (as such) overnight in a round-bottomed flask at bp under reflux. This gave also a white precipitate in a colourless solution. PXD and TG showed that the product was crystalline $TeO_3{\cdot}xH_2O$. This indicates that the dissolved species in the acid are effectively speaking H_6TeO_6(solv) that undergoes dehydration on prolonged heating.

The findings are summarized in Table 1. The present study constitutes the first systematic exploration of the reaction between H_6TeO_6 and H_2SO_4 with regard to variation of H_2SO_4 concentration, reaction temperature and duration. As seen from Table 1 the only effect of this treatment is dehydration of H_6TeO_6. TeO_3 (II) and $TeO_3{\cdot}xH_2O$ constitute new crystalline phases obtained by our treatment. TeO_3 (I) was earlier[32] prepared in an H_2SO_4 enviroment in a closed system. A natural question is why the valence state VI for tellurium stabilizes TeO_3 in conc. H_2SO_4 rather than a sulfate or an oxide sulfate. Although sulfates and oxide sulfates of elements in oxidation state VI are rare, they do exist, *e.g.* for $MoO_2(SO_4)$.[9,10] It is therefore not a general valence or crystal chemical rule which forbids formation of tellurium(VI) sulfate or oxide sulfate, but rather the thermodynamic stability of the various polymorphs of TeO_3.

Tellurium(IV) oxide or chloride as reactant

$Te_2O_3(SO_4)$ is the only solid product obtained from reaction between TeO_2 and 30–95 wt% H_2SO_4 at bp, or $TeCl_4$ and 60–80 wt% H_2SO_4 at bp and 85–95 wt% H_2SO_4 at 190 °C. In general the yield and reaction rate increase with increasing H_2SO_4 concentration and heating temperature. The best yields are obtained at bp. Derived unit-cell dimensions (Table 2) correspond to those reported for $Te_2O_3(SO_4)$.[50–52]

The reaction progresses differently for TeO_2 or $TeCl_4$ as reactant. In the case of TeO_2 a stage with complete dissolution to a clear, colourless solution was only obtained with ≤50 wt% H_2SO_4. For higher H_2SO_4 concentrations and above *ca.* 125 °C the dissolution of TeO_2 and precipitation of $Te_2O_3(SO_4)$ run in parallel. In the case of $TeCl_4$ as reactant a clear yellow solution is seen as the first step in the reaction, followed by a change to a colourless solution and eventually to the deposition of a white precipitate.

These findings together with experience from corresponding[6,8] reaction systems have led us to propose the following tentative reaction schemes. With TeO_2 as reactant, eqns. (1)–(3). With $TeCl_4$ as reactant, eqns. (4) and (5). In turn, eqn. (5)

$$2TeO_2(s) + H_2SO_4 \longrightarrow Te_2O_3^{2+}(solv) + H_2O(solv) + SO_4^{2-}(solv) \quad (1)$$

$$Te_2O_3^{2+}(solv) + SO_4^{2-}(solv) \longrightarrow Te_2O_3(SO_4)(solv) \quad (2)$$

$$Te_2O_3(SO_4)(solv) \longrightarrow Te_2O_3(SO_4)(s) \quad (3)$$

$$2TeCl_4(s) + 4H_2SO_4 \longrightarrow 2Te^{4+}(solv) + 8HCl(g) + 4SO_4^{2-}(solv) \quad (4)$$

$$2Te^{4+}(solv) + 3H_2O(solv) \longrightarrow Te_2O_3^{2+}(solv) + 6H^+(solv) \quad (5)$$

is followed by eqns. (2) and (3). The tentative character of eqns. (1)–(5) must be emphasized. It is experimentally documented that acidic fumes of HCl escape through the reflux

cooler during the syntheses with $TeCl_4$ [eqn. (4); no trace of SO_3(g) was detected in the exhaust gas].

Elemental tellurium as reactant

$Te_2O_3(SO_4)$ is the only solid product obtained in reactions between Te and 65–95 wt% H_2SO_4 at various temperatures. This is the old, original method (*cf.* Gmelin[47]) for synthesis of $2TeO_2{\cdot}SO_3 \equiv Te_2O_3(SO_4)$. The reaction rate increases appreciably with increasing H_2SO_4 concentration and reaction temperature (as also found for TeO_2 and $TeCl_4$ as reactants). With 95 wt% H_2SO_4 small amounts of $Te_2O_3(SO_4)$ are found at r.t., but the reaction rate is low and the yield is very poor. Conversely, no reaction is observed with 60 wt% H_2SO_4 in the temperature range r.t.–bp.

The progressing reaction between Te and 80–95 wt% H_2SO_4 at 100–200 °C is evidenced by dissolution of Te, liberation of SO_2 and a resulting red-violet solution, which turns weakly yellow to colourless and eventually a white deposit of $Te_2O_3(SO_4)$ separates. On adding glacial acetic acid to the violet solution (at r.t.) a black precipitate of elemental tellurium is formed. With 95 wt% H_2SO_4 the advancing reaction is easily recognized at 100 °C and is so vigorous at 200 °C that the three stages quickly merge into one another. With 85 wt% H_2SO_4 the reaction is quite slow at 100 °C, but much faster at 180 °C. According to Paul *et al.*[58] (and work quoted) the red-violet colour originates from Te_4^{2+}(solv) species which become oxidized (rate depending on temperature) to Te_2^{2+}(solv). The tentative reaction scheme (for 80–95 wt% H_2SO_4) in eqns. (6)–(8) is proposed which in turn is followed by eqns. (5), (2) and (3).

$$4Te(s) + 2H^+(solv) + H_2SO_4 \longrightarrow Te_4^{2+}(solv) + SO_2(g) + 2H_2O(solv) \quad (6)$$

$$Te_4^{2+}(solv) + 2H^+(solv) + H_2SO_4 \longrightarrow 2Te_2^{2+}(solv) + SO_2(g) + 2H_2O(solv) \quad (7)$$

$$Te_2^{2+}(solv) + 2H^+(solv) + H_2SO_4 \longrightarrow Te^{4+}(solv) + SO_2(g) + 2H_2O(solv) \quad (8)$$

In the concentration range 65–75 wt% H_2SO_4 the overall reaction rate is very much lower and the yield correspondingly poorer. However, the most prominent distinction is that the solution remains colourless right up to the moment $Te_2O_3(SO_4)$ commences to separate. The authors lean towards the view that the overall reaction scheme remains unchanged (see above), but that the relative reaction rates of eqns. (6)–(8) have changed dramatically. Hence, the dissolution reaction [eqn. (6)] in 80–95 wt% H_2SO_4 has become much slower than the subsequent reactions according to eqns. (7) and (8) (in particular the latter) in 65–75 wt% H_2SO_4.

Behaviour of reaction products towards water

None of the prepared tellurium compounds is appreciably hygroscopic and most are indifferent to a few days exposure to water. However, H_6TeO_6 and $TeO_3{\cdot}xH_2O$ are soluble in water and $Te_2O_3(SO_4)$ reacts with water to give TeO_2 and H_2SO_4, *cf.* Gmelin.[47]

Monoclinic H_6TeO_6 is recovered phase pure at r.t. after slow evaporation of an aqueous (colourless) solution of the dissolved acid. A similar treatment of a solution of $TeO_3{\cdot}xH_2O$ gave a mixture of monoclinic H_6TeO_6 and some 25 wt% of a largely amorphous material, $TeO_3{\cdot}xH_2O$ ($x \leq 3$).

The TeO_2 product usually obtained in admixture with $Te_2O_3(SO_4)$, after reaction between $Te_2O_3(SO_4)$ and water, proved not to be the tetragonal, thermodynamically stable form of TeO_2 (used as the starting reactant; see above), but rather the orthorhombic form (Table 2). This illustrates how a quasi-reversible cycle with H_2SO_4 as a reaction medium may (in certain cases) be utilized to prepare metastable oxides.

The products obtained from the reaction between $Te_2O_3(SO_4)$ and water are not fully reproducible. In several cases the products proved to be a mixture of tetragonal, orthorhombic and a third form of TeO_2 [here named γ-TeO_2; PXD reflections observed at d/pm = 349.6 (100), 306.8 (30), 303.4 (35), 232.76 (25), 228.42 (5) and 173.40 (25%)]. In some parallel experiments γ-TeO_2 coexisted with $Te_2O_3(SO_4)$.

Effect of heat treatment on the reaction products

Thermal stability ranges and relative mass losses for decomposition reactions were established by DTA and TG and are summarized in Table 3. The TG, DTG and DTA (DSC) scans for H_6TeO_6, TeO_3 (I), TeO_3 (II) and $Te_2O_3(SO_4)$ are shown in Figs. 1–3 as examples of simple and more complex decomposition courses. The agreement between observed and

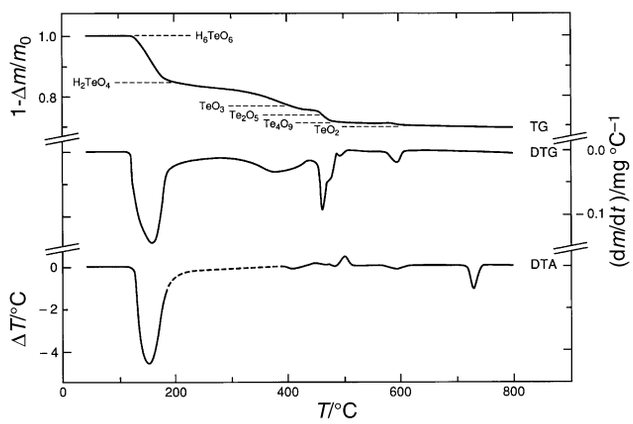

Fig. 1 TG, DTG and DTA data for H_6TeO_6. The DTA scan is adjusted to a constant background signal.

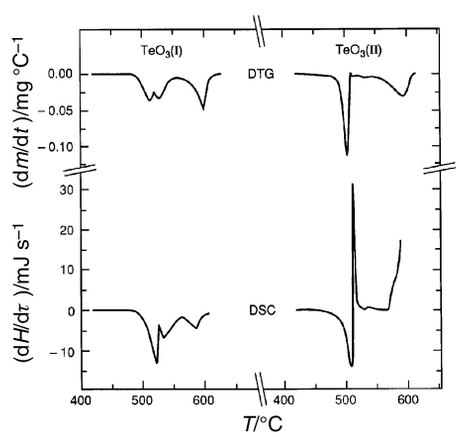

Fig. 2 DTG and DSC data (450–620 °C) for TeO_3 (I) and TeO_3 (II).

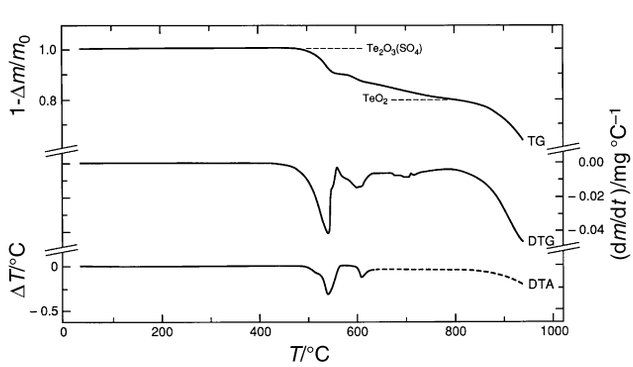

Fig. 3 TG, DTG and DTA data for $Te_2O_3(SO_4)$. The DTA scan is adjusted to a constant background signal.

Table 3 Summary of TG results for phase-pure reaction products, where m_0 refers to the mass at the start of the appropriate decomposition reaction

Compound	Decomposition reaction		T_{start}/°C	T_{end}/°C	$(\Delta m/m_0)_{obs}$	$(\Delta m/m_0)_{calc}$
H_6TeO_6	$H_6TeO_6(s) \longrightarrow H_2TeO_4(s) + 2H_2O(g)$	(9)	120	215	0.156	0.157
	$H_2TeO_4(s) \longrightarrow TeO_2(s) + H_2O(g) + \frac{1}{2}O_2(g)$	(10)	215	615	0.176	0.175
	$H_6TeO_6(s) \longrightarrow TeO_2(s) + 3H_2O(g) + \frac{1}{2}O_2(g)$	(9 + 10)	120	615	0.303	0.304
H_2TeO_4 [a]	Eqn. (10)		215	615	0.180	0.175
$TeO_3 \cdot xH_2O$ [b]	$TeO_3 \cdot xH_2O(s) \longrightarrow TeO_3(s) + xH_2O(g)$	(11)	215	405	0.105	—
	$TeO_3(s) \longrightarrow TeO_2(s) + \frac{1}{2}O_2(g)$	(12)	405	615	0.091	0.091
	$TeO_3 \cdot xH_2O(s) \longrightarrow TeO_2(s) + xH_2O(g) + \frac{1}{2}O_2(g)$	(11 + 12)	215	615	0.185	—
TeO_3 (I) [b,c]	$2TeO_3(s) \longrightarrow Te_2O_5(s) + \frac{1}{2}O_2(g)$	(13)	475	540	0.049	0.046
	$Te_2O_5(s) \longrightarrow 2TeO_2(s) + \frac{1}{2}O_2(g)$	(14)	540	615	0.051	0.048
	$TeO_3(s) \longrightarrow TeO_2(s) + \frac{1}{2}O_2(g)$	(13 + 14)	475	615	0.095	0.091
TeO_3 (II) [b,c]	Eqn. (13)		460	510	0.052	0.046
	Eqn. (14)		510	615	0.050	0.048
	Eqn. (13 + 14)		460	615	0.099	0.091
TeO_3 (III) [b]	Eqn. (13)		410	500	0.047	0.046
	Eqn. (14)		500	615	0.048	0.048
	Eqn. (13 + 14)		410	615	0.093	0.091
Te_2O_5 [d]	Eqn. (14)		540	615	0.045	0.048
Te_4O_9 [e]	$Te_4O_9(s) \longrightarrow 4TeO_2(s) + \frac{1}{2}O_2(g)$	(15)	515	630	0.022	0.024
$Te_2O_3(SO_4)$ [f]	$Te_2O_3(SO_4)(s) \longrightarrow 2TeO_2(s) + SO_3(g)$	(16)	450	785	0.200	0.200

[a] Prepared from H_6TeO_6 by heat treatment at 160 °C for 5 days; see Fig. 1. [b] For preparation see text and Table 1. [c] See Fig. 2. [d] Prepared from TeO_3 (I) by heat treatment at 490 °C for 15 h. [e] Prepared from H_6TeO_6 by heat treatment at 450 °C for 5 h. [f] See Fig. 3.

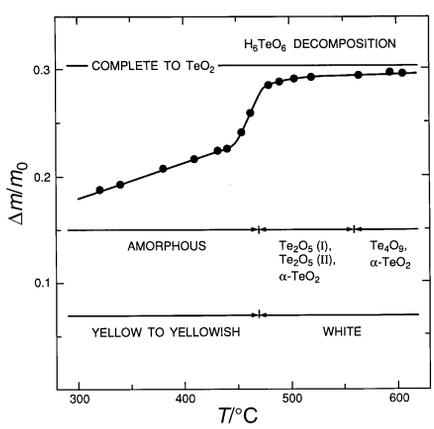

Fig. 4 Relative mass loss (in TG instrument) during thermal decomposition of H_6TeO_6 as a function of maximum set heating temperature. The colour and structural state of the reaction products are indicated.

calculated $\Delta m/m_0$ values (Table 3) is generally good and the TG data accordingly serve to confirm the composition of the various compounds.

The onset of the degradation of H_6TeO_6 to H_2TeO_4 (Table 3) is reasonably well defined in Fig. 1, whereas the further degradation to α-TeO_2 takes place over a broad temperature range and consists of several steps. This broad feature agrees with the earlier findings outlined in the Introduction, but the details differ to some extent.

Additional instructive results were obtained by heating H_6TeO_6 to a predecided temperature in the TG instrument and afterwards examining the products by PXD. The findings are summarized in Fig. 4. Although the $\Delta m/m_0$ *vs.* T relationship (Fig. 4) is regular, PXD shows that the intermediate crystalline products which appear during the decomposition are two- or three-phase mixtures. These findings were supplemented by experiments performed as a function of time at fixed temperatures. Under such conditions the temperature for the occurrence of crystalline products (470 °C in TG runs) is shifted to lower values. Heating, at say 450 °C, shows indications of crystalline intermediates after about 3/4 h. After 5 to 30 h mixtures containing Te_2O_5 (I), Te_2O_5 (II), Te_4O_9 and α-TeO_2 are clearly identified. As time progresses Te_2O_5 (I), Te_2O_5 (II) and Te_4O_9 gradually disappear, first Te_2O_5 (II) (after *ca.* 40 h at 450 °C) and then Te_2O_5 (I) (after *ca.* 3 days at 450 °C), whereas remains of Te_4O_9 are seen even after 17 days at 450 °C.

The coincidence of four entangled circumstances contributes to the complex thermal decomposition course of H_6TeO_6: (i) the initial decomposition products (at least H_2TeO_4 and TeO_3) are amorphous; (ii) the decomposition temperatures for the involved phases are lumped together within a rather narrow temperature range; (iii) the crystallization temperature for the intermediates (TeO_3, Te_2O_5, Te_4O_9 and perhaps H_2TeO_4) and TeO_2 falls within the domain of (i) and (ii); (iv) the crystallization process is exothermic (see, *e.g.*, Fig. 1; DTA *ca.* 430–515 °C), which adds complications to the signal deconvolution. (The crystallization of some amorphous phase(s) may generate extra heat which promotes further decomposition.) In conclusion the thermal decomposition of H_6TeO_6 appears to be ruled more by kinetic effects than by equilibrium thermodynamics.

The thermal decompositions of TeO_3 (I, II or III) and $TeO_3 \cdot xH_2O$ ($x = 1.37$–1.58) are summed up as two-stage reactions in Table 3, whereas those for H_2TeO_4, Te_2O_5, Te_4O_9 and $Te_2O_3(SO_4)$ are listed as one-step reactions. The actual processes are clearly more complex (see Figs. 1–4).

According to Table 3 the three modifications of TeO_3 differ somewhat in the onset and end temperatures for the reaction stages. Fig. 4 shows that Te_4O_9 may occur as an intermediate decomposition product of TeO_3 (I). The exothermic peaks which appear in the DSC scans for TeO_3 (II) and TeO_3 (III) reflect their metastable nature, and contribute to mask possible additional intermediate decomposition steps for these polymorphs. Similar findings were reported [30] earlier for TeO_3 (III).

The thermal decomposition (*cf.* TG data in Fig. 3) of $Te_2O_3(SO_4)$ was studied in more detail by heating samples at fixed temperatures. In one series, heat treatment at 550 °C for 15 h gave, after cooling to r.t., one-piece solidified product, implying that a major part of the sample had been in the molten state, findings in close agreement with Ref. 49. The product contained a mixture of $Te_2O_3(SO_4)$ and TeO_2 (*ca.* 30 wt% according to TG). At 580 °C TeO_2 had become the major phase of the corresponding mixture. The onset of the combined decomposition and melting of $Te_2O_3(SO_4)$ is observed at 450 °C by TG (Fig. 3 and Table 3). The DTA and DTG curves in Fig. 3 reflect the melting process in $Te_2O_3(SO_4)$–TeO_2 mixtures of variable composition and the DTA peak at *ca.* 610 °C

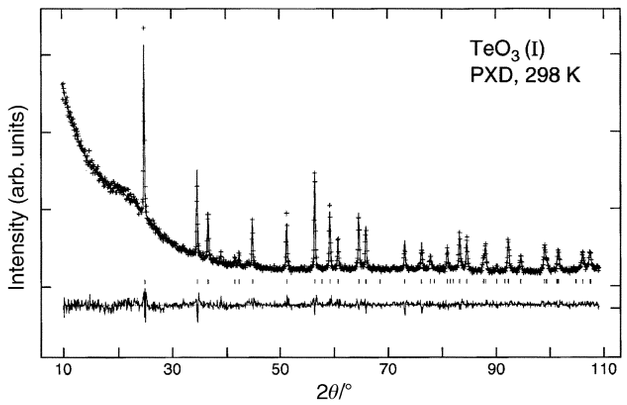

Fig. 5 Rietveld refinements (upper line) of PXD data (crosses; 6366 data points; 39 Bragg reflections) for TeO_3 (I). Positions of Bragg reflections are marked with bars. The difference between observed and calculated intensities is shown by the bottom line.

may possibly be a manifestation of the melting of TeO_2 in such a eutectic-like mixture. Pure TeO_2 melts at about 730 °C according to the present DTA data (Fig. 1) in good agreement with the literature[21] value of 733 ± 1 °C. Fig. 3 shows furthermore that TeO_2 sublimes above *ca.* 800 °C. The occurrence of the molten $Te_2O_3(SO_4)$–TeO_2 mixtures constitutes a considerable obstacle for a more detailed insight into the thermal decomposition of $Te_2O_3(SO_4)$.

Redetermined crystal structure of TeO_3 (I)

The crystal structure of TeO_3 (I) was redetermined before we had discovered the work of Dušek and Loub.[37] The unit-cell dimensions given in Table 2 are (perhaps owing to different methods of preparation) somewhat larger than those reported in Refs. 32 and 37. The positional parameter of Dumora and Hagenmuller[32] was used as input parameter for the Rietveld refinements and these converged nicely to $R(F^2) = 0.095$, $R_{wp} = 0.065$, $R_p = 0.045$ and $\chi^2 = 2.16$, see Fig. 5. TeO_3 (I) crystallizes in space group $R\bar{3}c$, and in terms of the rhombohedral description Te is located in 2*b* (000) and O in 6*e* (x, $\frac{1}{2} - x$, $\frac{1}{4}$) with $x = 0.892(1)$ [$U_{iso}/100 = 1.4(1)$ and $1.0(2)$ pm^2 for Te and O, respectively]. The present value for x compares quite favourably with that of Dušek and Loub[37] [$x = 0.890(6)$], but differs from the approximate value of Dumora and Hagenmuller[32] ($x = 0.85$).

The present values for the structural variables a, a and x give 191.8(3) pm for the Te–O bond, 357.32(1) pm for the shortest interatomic Te···Te distance and 89.05(7) and 137.4(4)° for the angles O–Te–O and Te–O–Te, respectively. An illustration of the TeO_3 (I) structure is given in Ref. 37.

Redetermined crystal structure of $Te_2O_3(SO_4)$

The object of the redetermination of the crystal structure of $Te_2O_3(SO_4)$ was to provide more accurate positional parameters for the oxygen atoms. However, during the work it became obvious that there are inconsistencies between the parameters reported in Refs. 50–52, possibly owing to trivial errors during compilation of the crystallographic data (*cf.* Ref. 53).

Diffractometer PND data for $Te_2O_3(SO_4)$ were collected at r.t. The unit-cell dimensions in Table 2 agree closely with Refs. 50 and 52, whereas they are systematically smaller than those of Loub *et al.*[51] The positional parameters of Johansson and Lindqvist[50] were used as input for the Rietveld refinements (space group $Pmn2_1$, standard setting). These calculations converged to the positional parameters listed in Table 4 [$R(F^2) = 0.073$, $R_{wp} = 0.059$, $R_p = 0.046$, $\chi^2 = 2.90$; Fig. 6]. The present values are in good to reasonable agreement with those of Johansson and Lindqvist[50] except for the z parameter

Table 4 Positional parameters (space group $Pmn2_1$; calculated standard deviations in parentheses) for $Te_2O_3(SO_4)$ at r.t. according to Ritveld refinements of PND data. For unit-cell dimensions see Table 2. Refined values for $U_{iso}/100$ are 0.65, 0.27 and 0.91 pm^2 for Te, S and O, respectively. The positional parameters listed in Ref. 53 (in italics) are quoted for comparison

Atom	Site	x	y	z
Te	4*b*	0.3013(2)	0.6782(3)	1/4
		0.3008	*0.6782*	*1/4*
S	2*a*	0	0.0182(6)	0.329(1)
		0	*0.0210*	*0.3270*
O(1)	4*b*	0.3624(3)	0.9495(3)	0.0062(7)
		0.365	*0.946*	*−0.003*
O(2)	2*a*	0	0.1595(5)	0.0915(8)
		0	*0.166*	*0.089*
O(3)	2*a*	0	0.4121(5)	0.6622(8)
		0	*0.416*	*0.648*
O(4)	4*b*	0.2365(3)	0.5929(3)	0.8827(7)
		0.261	*0.406*	*0.377*
O(5)	2*a*	0	0.8181(5)	0.2282(8)
		0	*0.825*	*0.207*

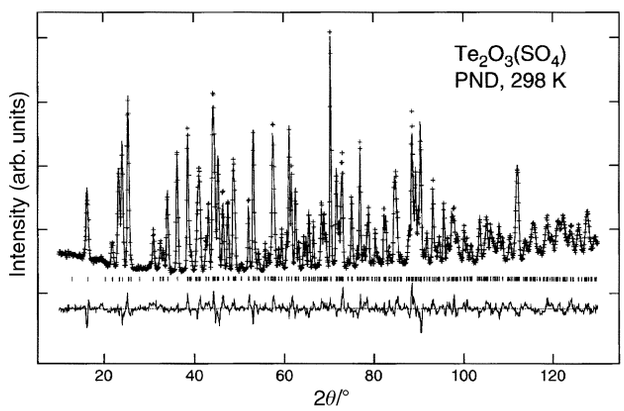

Fig. 6 Rietveld refinements (upper line) of PND data (crosses; $\lambda = 155.4$ pm; 2403 data points; 292 Bragg reflections) for $Te_2O_3(SO_4)$. Positions of Bragg reflections are marked with bars. The difference between observed and calculated intensities is shown by the bottom line.

of atom O(4) (which is related to the present value by $1 - z$). In order not to add to the confusion concerning $Te_2O_3(SO_4)$, Table 4 uses the same origin and numbering of the atoms as Ref. 53. As seen from the table the previous coordinates for O(4) appear to be related to the present values by $\frac{1}{2} - x$, $1 - y$, $\frac{5}{4} - z$. Note that PND data are very sensitive to the oxygen scattering and this explains the rather large numerical mismatch with the earlier[50–53] reported X-ray-diffraction-based oxygen coordinates, in particular the O(4) parameters.

Relevant interatomic distances and angles for the redetermined $Te_2O_3(SO_4)$ crystal structure are given in Table 5. Illustrations of the structure are found in Refs. 50–53. The main distinction between the presently redetermined coordinates and those of Refs. 50–52 concerns O(4) (for mutual distinctions between Refs. 50–52, see Ref. 53). The effect of the new coordinates for O(4) is that the Te–O(4)–Te [Te–O(4′)–Te] bridges within the puckered $Te_2O_3^{2+}$ layers change appearance in a mirror-image-like manner (see Fig. 7).

Bond valences

Bond valences (V_i) for relevant tellurium compounds have been calculated from observed interatomic distances (d_{ij}/100 pm) according to expression[59] (17) where D_{ij} is the bond valence

$$V_i = \Sigma_j \exp[(D_{ij} - d_{ij})/b] \quad (17)$$

Table 6 Bond valence data for tellurium oxygen-containing compounds (averages in italics)

Compound	Bond valence (V_i) Specification	Range	Sum	Average	Oxidation state	Ref.
H_6TeO_6 (monoclinic)	Te(1)–O	1.019–1.027	6.14			
	Te(2)–O	1.008–1.024	6.11	*6.12*	6	22
H_6TeO_6 (cubic)	Te–O	1.81–1.98	6.51		6	23
H_2TeO_4	Te–O	0.97–1.04	6.08		6	24
TeO_3 (I)	Te–O	0.999	6.00		6	Present
$H_2Te_2O_6$	Te(1)–O	0.91–1.15	6.01			
	Te(2)–O	0.09–1.37	4.16	*5.08*	5	20
Te_2O_5	Te(1)–O	0.86–1.21	6.00			
	Te(2)–O	0.14–1.26	4.10	*5.05*	5	17
Te_4O_9	Te(1)–O	0.92–1.04	5.88			
	Te(2)–O	0.10–1.29	4.04	*4.50*	4.5	16
α-TeO_2 (tetragonal)	Te–O	0.675–1.307	3.96		4	12
β-TeO_2 (orthorhombic)	Te–O	0.17–1.30	3.95		4	13
$Te_2O_3(SO_4)$	Te–O	0.167–1.248	3.99		4	
	S–O	1.421–1.520	5.85		6	Present

Table 5 Relevant interatomic distances (in pm) and angles (in °) in the redetermined crystal structure of $Te_2O_3(SO_4)$. Calculated standard deviations are given in parentheses

Te–O(1)	226.3(3)	S–O(1)	149.1(3)
Te–O(2)	262.8(3)	S–O(1′)	149.1(3)
Te–O(3)	191.7(3)	S–O(2)	147.8(4)
Te–O(4)	189.8(3)	S–O(5)	146.5(5)
Te–O(4′)	200.7(3)		
Te–O(5)	284.8(2)		
O(1)–Te–O(2)	77.6(1)	O(1)–S–O(1′)	110.1(3)
O(1)–Te–O(3)	86.8(1)	O(1)–S–O(2)	108.3(2)
O(1)–Te–O(4)	83.1(1)	O(1)–S–O(5)	108.7(2)
O(1)–Te–O(4′)	166.7(1)	O(1′)–S–(2)	108.3(2)
O(1)–Te–O(5)	85.7(1)	O(1′)–S–O(5)	108.7(2)
O(2)–Te–O(3)	69.5(1)	O(2)–S–O(5)	112.9(4)
O(2)–Te–O(4)	151.8(1)		
O(2)–Te–O(4′)	109.1(1)	Te–O(1)–S	126.8(2)
O(2)–Te–O(5)	120.5(1)	Te–O(2)–Te	84.4(1)
O(3)–Te–O(4)	89.1(1)	Te–O(2)–S	137.4(7)
O(3)–Te–O(4′)	85.0(1)	Te–O(3)–Te	134.1(2)
O(3)–Te–O(5)	165.7(1)	Te–O(4)–Te	128.3(1)
O(4)–Te–O(4′)	86.2(1)	Te–O(5)–S	140.0(1)
O(4)–Te–O(5)	77.9(1)	Te–O(5′)–S	108.1(1)
O(4′)–Te–O(5)	100.0(1)		

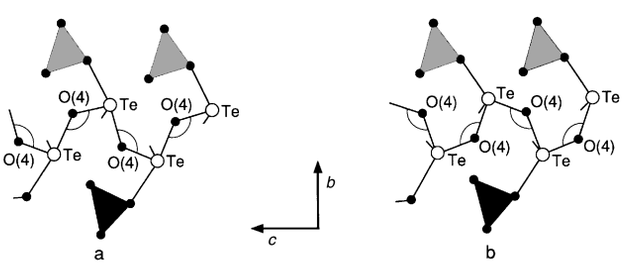

Fig. 7 Segment of a tellurium–oxygen layer of the $Te_2O_3(SO_4)$ structure according to (a) the present results and (b) Ref. 53.

parameter for the type of bond concerned and $b = 0.37$. For the compounds of current interest, Ref. 59 lists $D_{ij} = 1.917$, 1.977 and 1.624 for Te^{VI}–O, Te^{IV}–O and S^{VI}–O, respectively. The bond valences in Table 6 show a generally good match with formal oxidation numbers.

Used in this (common) way, the derived bond valence becomes merely a kind of auditing parameter which reflects the chemical reliability of the crystal structure. The decisive power of such auditing tests clearly also depends on the correctness of the parameters D_{ij} and b. The close correspondence between the two kinds of valence data in Table 6 gives some kind of quality confirmation for both the bond valence parameters involved and the crystal structure determination concerned. The only one of these structures which may be worthwhile to redetermine appears to be H_6TeO_6(cubic).

Acknowledgements

This project has received financial support from the Research Council of Norway (NFR).

References

1 K. Selte and A. Kjekshus, *Acta Chem. Scand.*, 1970, **24**, 1912.
2 S. Furuseth, K. Selte, H. Hope, A. Kjekshus and B. Klewe, *Acta Chem. Scand.*, *Ser. A*, 1974, **28**, 71.
3 M. A. K. Ahmed, H. Fjellvåg and A. Kjekshus, *Acta Chem. Scand.*, 1994, **48**, 537.
4 H. Fjellvåg and A. Kjekshus, *Acta Chem. Scand.*, 1994, **48**, 815.
5 M. A. K. Ahmed, H. Fjellvåg and A. Kjekshus, *Acta Chem. Scand.*, 1995, **49**, 457.
6 M. A. K. Ahmed, H. Fjellvåg and A. Kjekshus, *Acta Chem. Scand.*, 1996, **50**, 275.
7 M. A. K. Ahmed, H. Fjellvåg and A. Kjekshus, *Acta Chem. Scand.*, 1998, **52**, 305.
8 M. A. K. Ahmed, H. Fjellvåg and A. Kjekshus, *Acta Chem. Scand.*, 1999, **53**, 24.
9 A. F. Christiansen, H. Fjellvåg and A. Kjekshus, *J. Chem. Soc.*, *Dalton Trans.*, submitted.
10 A. F. Christiansen, H. Fjellvåg and A. Kjekshus, *J. Chem. Soc.*, *Dalton Trans.*, submitted.
11 *Gmelin Handbuch der anorganischen Chemie*, System-Nummer 11, Tellur, Ergänzungsband B1–3, Springer, Berlin, 1976–1978.
12 W. R. McWhinnie, in *Encyclopedia of Inorganic Chemistry*, Chief ed. R. B. King, Wiley, Chichester, 1994, p. 4105.
13 J. Leciejewicz, *Z. Kristallogr.*, 1961, **116**, 345.
14 O. Lindqvist, *Acta Chem. Scand.*, 1968, **22**, 977.
15 I. P. Kondratyuk, L. A. Muradyan, Yu. V. Pisarevskii and V. I. Simonov, *Kristallografiya*, 1987, **32**, 609.
16 P. A. Thomas, *J. Phys. C: Solid State Phys.*, 1988, **21**, 4611.
17 T. Ito and H. Swada, *Z. Kristallogr.*, 1939, **102**, 13.
18 H. Beyer, *Z. Kristallogr.*, 1967, **124**, 228.
19 T. G. Worlton and R. A. Beyerlein, *Phys. Rev. B*, 1975, **12**, 1899.
20 E. F. Skelton, J. L. Feldman, C. Y. Liu and I. L. Spain, *Phys. Rev. B*, 1976, **13**, 2605.
21 V. P. Itkin and C. B. Alcock, *J. Phase Equilib.*, 1996, **17**, 533.
22 L. A. Demina, I. A. Khodyakova, V. A. Dolgikh, O. I. Vorobeva and A. V. Novoselova, *Russ. J. Inorg. Chem.*, 1981, **26**, 312.
23 J. Moret and O. Lindqvist, *C. R. Acad. Sci.*, *Ser. C*, 1972, **275**, 207.
24 O. Lindqvist, W. Mark and J. Moret, *Acta Crystallogr.*, *Sect. B*, 1975, **31**, 1255.
25 J. Rosicky, J. Loub and J. Pavel, *Z. Anorg. Allg. Chem.*, 1965, **334**, 312.
26 O. Lindqvist and J. Moret, *Acta Crystallogr.*, *Sect. B*, 1973, **29**, 643.
27 J. Moret and M. Maurin, *C. R. Acad. Sci.*, *Ser. C*, 1968, **266**, 708.
28 M. Patry, *Bull. Soc. Chim. Fr.*, 1936, 845.
29 M. Montignie, *Bull. Soc. Chim. Fr.*, 1947, 564.
30 J. Loub, *Z. Anorg. Allg. Chem.*, 1968, **362**, 98.

31 M. Maurin and J. Moret, *C. R. Acad. Sci.*, *Ser. C*, 1968, **266**, 22.
32 D. Dumora and P. Hagenmuller, *C. R. Acad. Sci.*, *Ser. C*, 1968, **266**, 276.
33 J. Loub and J. Rosicky, *Z. Anorg. Allg. Chem.*, 1969, **365**, 308.
34 J. C. J. Bart, A. Bossi, P. Perissinoto, A. Castellan and N. Giordano, *J. Therm. Anal.*, 1975, **8**, 313.
35 J. Loub, *Collect. Czech. Chem. Commun.*, 1977, **42**, 960.
36 C. P. Marin, M. L. V. Blanco and E. G. Rios, *An. Quim.*, 1977, **73**, 816.
37 M. Dušek and J. Loub, *Powder Diffr.*, 1988, **3**, 175.
38 O. N. Breusov, O. I. Vorobjeva, A. N. Druz, T. V. Rovzina and B. R. Sobolev, *Izv. Akad. Nauk SSSR, Neorg. Mater.*, 1966, **2**, 380.
39 J. Loub and J. Rosicky, *Z. Anorg. Allg. Chem.*, 1968, **361**, 87.
40 C. Pico, A. Jerez, M. L. Veiga and E. Gutierrez-Rios, *J. Therm. Anal.*, 1979, **15**, 191.
41 J. Fábry, J. Loub and L. Feltl, *J. Therm. Anal.*, 1982, **24**, 95.
42 O. Lindqvist and J. Moret, *Acta Crystallogr.*, *Sect. B*, 1973, **29**, 956.
43 O. Lindqvist, *Acta Chem. Scand.*, 1970, **24**, 3178.
44 O. Lindqvist and M. S. Lehmann, *Acta Chem. Scand.*, 1973, **27**, 85.
45 D. F. Mullica, J. D. Korp, W. O. Milligan, G. W. Beall and I. Bernal, *Acta Crystallogr.*, *Sect. B*, 1980, **36**, 2565.
46 J. Moret, E. Philippot, M. Maurin and O. Lindqvist, *Acta Crystallogr.*, *Sect. B*, 1974, **30**, 1813.
47 *Gmelins Handbuch der anorganischen Chemie*, System-Nummer 11, Tellur, 8-Aufl., Verlag Chemie, Berlin, 1940.
48 J. Loub and H. Hubkova, *Z. Chem.*, 1965, **5**, 341.
49 H. Hubkova, J. Loub and V. Synecek, *Collect. Czech. Chem. Commun.*, 1966, **31**, 4353.
50 G. B. Johansson and O. Lindqvist, *Acta Crystallogr.*, *Sect. B*, 1976, **32**, 2720.
51 J. Loub, J. Podlahová and C. Novák, *Acta Crystallogr.*, *Sect. B*, 1976, **32**, 3115.
52 H. Mayer and G. Pupp, *Monatsh. Chem.*, 1976, **107**, 721.
53 *Structure Reports*, eds. L. D. Calvert and J. Trotter, International Union of Crystallography, Utrecht, 1976, vol. 42A, p. 371.
54 P.-E. Werner, Program SCANPI-6, Institute of Inorganic Chemistry, Stockholm University, 1988.
55 P.-E. Werner, Program TREOR-5, Institute of Inorganic Chemistry, Stockholm University, 1988 [see also P. E. Werner, *Z. Kristallogr.*, 1964, **120**, 375].
56 N. O. Ersson, Program CELLKANT, Chemical Institute, Uppsala University, 1981.
57 A. C. Larson and R. B. Von Dreele, Program GSAS, General Structure Analysis System, LANSCE, MS-H 805, Los Alamos National Laboratory, Los Alamos, NM, 1998.
58 R. C. Paul, C. L. Arora, J. K. Puri, R. N. Virmani and K. C. Malhortra, *J. Chem. Soc.*, *Dalton Trans.*, 1972, 781.
59 N. E. Brese and M. O'Keeffe, *Acta Crystallogr.*, *Sect. B*, 1991, **47**, 192.